

# Integration Tests of the 4 kW-class High Voltage Hall Accelerator Power Processing Unit with the HiVHAc and the SPT-140 Hall Effect Thrusters

Hani Kamhawi<sup>1</sup>, Luis Pinero<sup>2</sup>, Thomas Haag<sup>3</sup>, Wensheng Huang<sup>4</sup>, and Drew Ahern<sup>5</sup>  
*National Aeronautics and Space Administration Glenn Research Center, Cleveland, Ohio, 44135*

Ray Liang<sup>6</sup>  
*Space Systems Loral, Palo Alto, California, 94303*

*and*

Vlad Shilo<sup>7</sup>  
*Colorado Power Electronics, Inc., Fort Collins, Colorado, 80542*

NASA's Science Mission Directorate is sponsoring the development of a 4 kW-class Hall propulsion system for implementation in NASA science and exploration missions. The main components of the system include the High Voltage Hall Accelerator (HiVHAc), an engineering model power processing unit (PPU) developed by Colorado Power Electronics, and a xenon flow control module (XFCM) developed by VACCO Industries. NASA Glenn Research Center is performing integrated tests of the Hall thruster propulsion system. This paper presents results from integrated tests of the PPU and XFCM with the HiVHAc engineering development thruster and a SPT-140 thruster provided by Space System Loral. The results presented in this paper demonstrate thruster discharge initiation along with open-loop and closed-loop control of the discharge current with anode flow for both the HiVHAc and the SPT-140 thrusters. Integrated tests with the SPT-140 thruster indicated that the PPU was able to repeatedly initiate the thruster's discharge, achieve steady state operation, and successfully throttle the thruster between 1.5 and 4.5 kW. The measured SPT-140 performance was identical to levels reported by Space Systems Loral.

## I. Introduction

Electric propulsion (EP) systems can enable and enhance NASA's ability to perform scientific space exploration. NASA Science Mission Directorate (SMD) planetary science missions to small bodies include fly-by, rendezvous, and sample return from a diverse set of targets.<sup>1</sup> For example, NASA missions have successfully employed EP systems on the Deep Space 1 (DS1) and Dawn missions.<sup>2,3</sup> To augment its capability to perform these and other solar system exploration missions, NASA continues to develop advanced EP technologies. Recent small body mission studies indicate that the majority of these small body missions are enabled by the use of EP, and nearly all of the small body missions of interest are enhanced with EP.

Electric propulsion system performance can significantly reduce launch vehicle requirements, costs, and spacecraft mass because of its high specific impulse capability when compared to chemical propulsion. A recent study found that significant cost savings can be realized by use of EP when compared to chemical propulsion for NASA Discovery class missions.<sup>4</sup>

---

<sup>1</sup> Senior Research Engineer, Electric Propulsion Systems Branch, AIAA Associate Fellow.

<sup>2</sup> Senior Research Engineer, Electric Propulsion Systems Branch, AIAA Senior Member.

<sup>3</sup> Senior Research Engineer, Electric Propulsion Systems Branch, AIAA Senior Member.

<sup>4</sup> Senior Research Engineer, Electric Propulsion Systems Branch, AIAA Senior Member.

<sup>5</sup> Research Engineer, Electric Propulsion Systems Branch, AIAA Student Member.

<sup>6</sup> Propulsion Specialist, Space Systems Loral, AIAA Member.

<sup>7</sup> Senior Engineer, Colorado Power Electronics Inc.

Mission studies evaluated the performance of the High Voltage Hall Accelerator (HiVHAc) 4-kW class thruster propulsion system for four NASA Discovery class design reference missions (DRMs) that included:

- Vesta-Ceres rendezvous mission (i.e., Dawn Mission), which has both time constraints and a very high post launch  $\Delta V$ , requiring both a moderate thrust-to-power and a higher specific impulse than a conventional Hall thruster;
- Koppf comet rendezvous mission, which has few constraints and does not require thruster operation in gravity wells (this favors a high specific impulse throttle table);
- Near-Earth Asteroid Return Earth Return (NEARER) mission; and
- Nereus sample return (NSR) mission, which is a relatively low  $\Delta V$  mission with time constraints favorable for a higher thrust-to-power thruster.

Results from the mission studies indicated that the HiVHAc propulsion system was able to exceed the needs of all the evaluated missions.

The NASA DRMs required the development of a new Hall propulsion system that can operate in two modes: high specific impulse and modestly high thrust-to-power. To attain high specific impulse and high thrust-to-power operation required a power processing unit (PPU) that supplies discharge voltages up to 700 V and discharge currents up to 15 A, while not exceeding a total discharge power of 4.5 kW. Additionally, NASA's science missions required a PPU that can operate at variable input voltage range to accommodate the spacecraft power management system's supplied voltage. To that end, NASA GRC is working with Colorado Power Electronics (CPE) to mature the design of a 4.5 kW PPU with an input voltage range of 70-140 V and an output voltage range of 200-700 V for implementation in NASA's HiVHAc propulsion system.<sup>5,6</sup>

This paper will present recent test results of the integrated tests of the CPE PPU and VACCO xenon flow control module (XFCM) with NASA's HiVHAc thruster and the SPT-140 Hall Effect Thruster (HET) provided by Space Systems Loral (SSL). The paper is arranged as follows: Section II presents an overview of the Hall thruster propulsion system under development and test, Section III presents results from the integrated tests with the HiVHAc thruster, Section IV presents results from integrated tests with the SPT-140, and Section V presents the summary and future work.

## II. Hall Propulsion System Overview

The major elements of the dual-mode long-life Hall propulsion system that is being developed and matured by NASA Glenn Research Center (GRC) include the HiVHAc thruster, PPU, and XFCM as is shown in Figure 1. NASA GRC is performing the thruster development and test activities. The HiVHAc project is utilizing a PPU that is being designed and developed by CPE. The XFCM was designed and developed by VACCO Industries.<sup>7</sup>

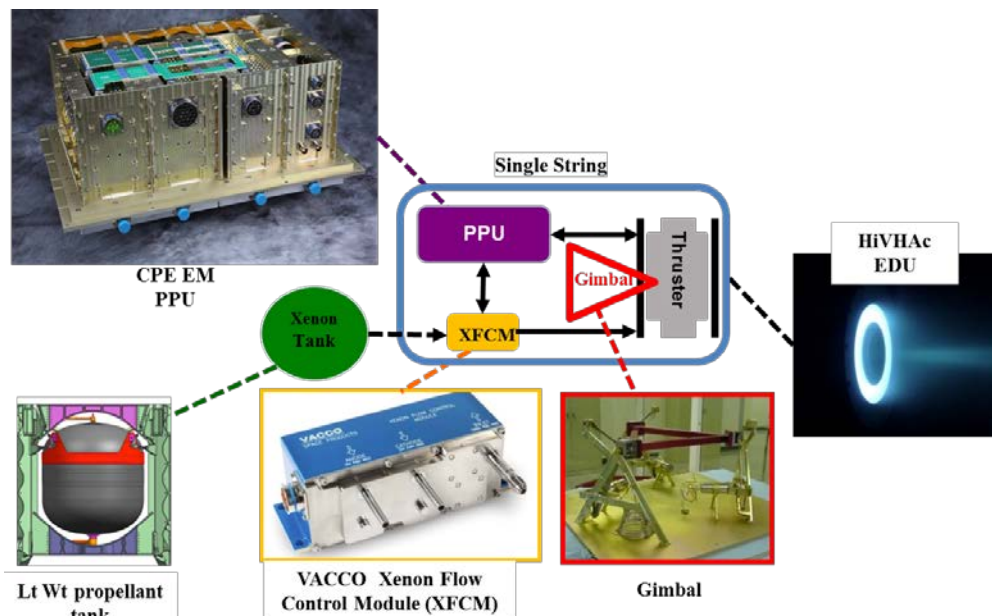


Figure 1: HiVHAc propulsion system layout showing the HiVHAc EDU, CPE EM PPU, and VACCO XFCM.

## A. Hall Effect Thruster

. Two thrusters were used in this study to demonstrate the full range of capabilities for both the PPU and XFCM and to show compatibility of the PPU and XFCM with different HETs, including a commercial-off-the-shelf unit (COTS). These two thrusters were the HiVHAc engineering development unit (EDU) and the SPT-140 development model 4 (DM4)

### 1. High Voltage Hall Accelerator

The HiVHAc EDU thruster, shown operating in Figure 1, was a joint development between NASA GRC and Aerojet-Rocketdyne. The thruster has undergone extensive performance and thermal characterization tests in addition to undergoing a random vibration test.<sup>8</sup> The EDU thruster is designed to operate at a peak discharge power of 3.9 kW at discharge voltages up to 650 V. The thruster incorporates an in-situ discharge channel replacement mechanism for life extension. The thruster development plan has been detailed in other publications.

### 2. Space Systems Loral SPT-140

The SPT-140 DM4 thruster was manufactured by Fakel Experimental Design Bureau and was provided on loan to NASA GRC by Space Systems Loral. The thruster is designed to operate at discharge power levels of 3 kW and 4.5 kW but can be throttled up to 6 kW. Tests of earlier versions of the SPT-140 were performed at NASA GRC by Manzella.<sup>9,10</sup> The thruster can operate at discharge voltages up to 600 V and discharge currents up to 20 A. For the present SPT-140 test campaign, the thruster's original cathode assemblies were replaced with a NASA GRC cathode assembly to enable hollow cathode heating and ignition using the built-in capability in the CPE EM PPU. The radial and axial location of the cathode keeper orifice was identical to the location of SPT-140's original lanthanum hexaboride cathodes. Figure 2 shows a photograph of the SPT-140 with NASA's cathode assembly inside vacuum facility 12 (VF12).



**Figure 2: SSL SPT-140 DM4 mounted with NASA cathode assembly on an inverted pendulum thrust stand in NASA GRC's VF12.**

## B. Colorado Power Electronics Engineering Model Power Processing Unit

The CPE HiVHAc EM PPU was developed to operate the HiVHAc thruster. Table 1 summarizes the input and output requirements for the EM PPU. This modular PPU consists of four modules including two discharge modules; an ancillary module for the inner magnet, outer magnet, keeper, and heater supplies; and a digital control interface unit (DCIU) module. The DCIU contains the controller board, XFCM driver board, and the housekeeping supply. The EM PPU mass is 15.6 kg and measures approximately 38.6 cm by 23.2 cm by 16.3 cm. A photograph of the PPU is shown in Figure 1. Extensive functional tests of the EM PPU have been performed at NASA GRC and are reported in an accompanying paper.<sup>6</sup>

**Table 1: CPE EM PPU electrical specifications.**

EM PPU	Discharge	Magnets (2)	Keeper	Heater
<b>Output Voltage</b>	200 – 700 V	2 – 10 V	5 – 40 V	1 – 15 V
<b>Output Current</b>	1.4 – 15 A	1 – 5 A	1 – 4 A	3.5 – 10 A
<b>Output Power Max</b>	4 kW	50 W	80 W	150 W
<b>Regulation Mode</b>	Voltage or Current	Current	Current	Current
<b>Output Ripple</b>	$\leq 5\%$			
<b>Line/Load Regulation</b>	$\leq 2\%$			
<b>Input Voltage</b>	80 – 160 V (main) and 24 – 34V (housekeeping)			

### C. VACCO Xenon Flow Control Module

The VACCO XFCM is the baseline xenon feed system for the HiVHAc propulsion system. The XFCM development was funded by NASA and the Air Force Research Laboratory. A block diagram of the XFCM is shown in Figure 3. The unit incorporates two redundant micro-latching valves, two piezoelectric control valves, passive flow restrictors, and input and output pressure and temperature transducers to enable flow rate calculation. The XFCM is capable of taking xenon directly from a tank at a pressure range of 10 to 3,000 psia and providing regulated flow at a range of 0 to 160 sccm for the anode and cathode. Table 2 summarizes the VACCO XFCM specifications.

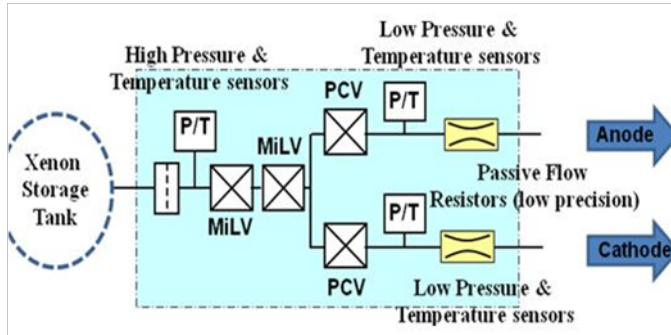


Figure 3. VACCO XFCM Block Diagram.

For this test campaign the XFCM was placed inside VF12. The XFCM setup in VF12, shown in Figure 4, includes five external solenoid valves to provide flexibility in delivering xenon to the thruster. The layout shown provides the option of bypassing the XFCM unit to enable supplying xenon directly from the laboratory mass flow controllers (MFCs) to the thruster's anode and cathode unit. The setup also provides the flexibility to use the XFCM unit to provide flow to the thruster while still supplying the cathode flow with the MFC.

Table 2. VACCO XFCM Specifications

Inlet Pressure Range	10 to 3000 psia
Anode Flow Range	0 to 160 sccm Xenon
Cathode Flow Range	0 to 160 sccm Xenon
Flow Accuracy	±3% of set value (closed loop)
Internal Leakage	$1.0 \times 10^{-3}$ scch GHe
External Leakage	$1.0 \times 10^{-6}$ sccs
Lifetime	10 years, 7,300 cycles, 100% margin
Mass	< 1.25 kg
Power Consumption	< 1 W steady state
Size (W×H×D)	19.5cm × 7.0 cm × 7.5 cm

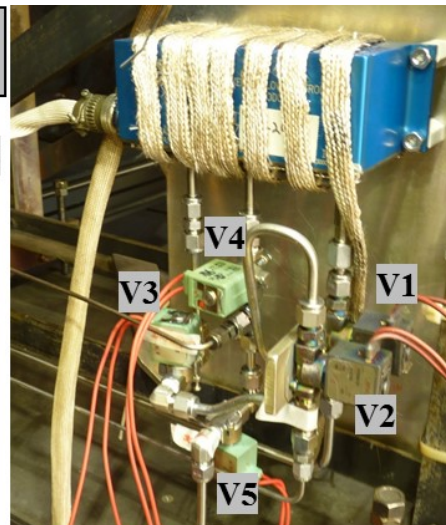
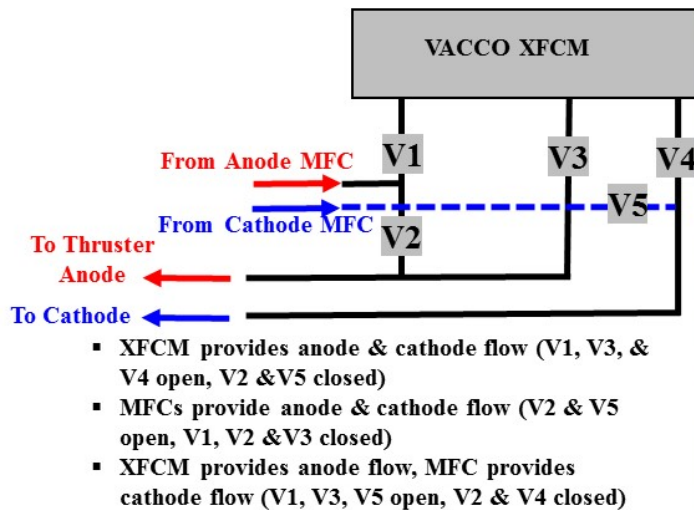


Figure 4. VACCO XFCM photograph in GRC VF-12 showing solenoid valves.



### III. HiVHAc Thruster Integration Test Results

Tests of the HiVHAc EDU were performed in VF12 at NASA GRC. Vacuum Facility 12 is a 3 m diameter, 9 m long cylindrical cryopumped facility with a pumping speed of approximately 450,000 L/sec (air). Recent tests of VF12 indicate a base pressure of  $8.9 \times 10^{-8}$  Torr. A background pressure of approximately  $3.3 \times 10^{-5}$  Torr (air) was attained at a xenon flow rate of 160 sccm. The walls of VF12 are lined with 1.3 cm thick graphite paneling to reduce the back-sputtered material flux to the thruster and test support hardware. In 2013, the HiVHAc thruster was integrated with the CPE brassboard PPU and the XFCM unit, and operation was demonstrated in an open-loop configuration.<sup>11</sup> For the present HiVHAc thruster tests, no thrust measurements were performed, consistent with the primary objective of demonstrating the closed-loop operation of the thruster with the PPU and XFCM units. In addition, the EM PPU was located outside of VF12 in air.

The primary objective of the HiVHAc thruster integration test during this test segment was demonstrating that the EM PPU was capable of the following: controlling the XFCM, heating the cathode, igniting the cathode, initiating the HiVHAc thruster discharge, maintaining steady-state thruster operation at the set discharge current level by regulating the anode flow, and performing thruster throttling. To achieve these objectives, operational algorithms were developed by NASA GRC and CPE. Tests with the HiVHAc thruster were used to refine the control algorithm parameters. Details of the discharge current feedback loop are presented in Reference 6.

The HiVHAc thruster discharge was initiated at 300 V and 2.5 A several times using two different thruster discharge initiation algorithms. Figures 5 and 6 show the discharge current, discharge voltage, magnet current, and anode flow profiles for initiating the thruster discharge in nominal Hall mode and glow mode, respectively. For both discharge initiation approaches, the cathode discharge was already on. For the Hall mode discharge initiation shown in Fig. 5, the thruster's magnets were energized and the discharge voltage was applied (at a specified ramp rate) as the anode flow was increased. After approximately 50 s, the discharge current reached its set magnitude. For the glow mode discharge initiation shown in Fig. 6, the anode flow is initiated, first resulting in discharge current initiation. As the discharge current reaches the PPU set current limit, the magnet current is ramped to its set value and the thruster's discharge starts transitioning to Hall mode. At that point, the PPU's DCIU proportional integral derivative (PID) loop ramps down the anode flow, and the thruster reaches its set discharge current and voltage magnitude in approximately 15 s.

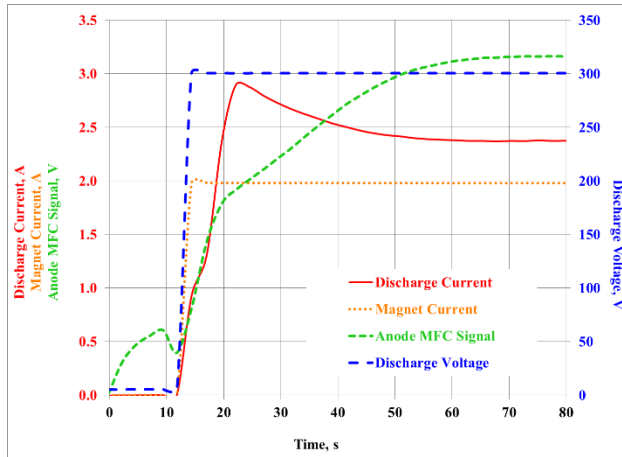


**Figure 5. Plot of the HiVHAc thruster nominal discharge initiation transient.**

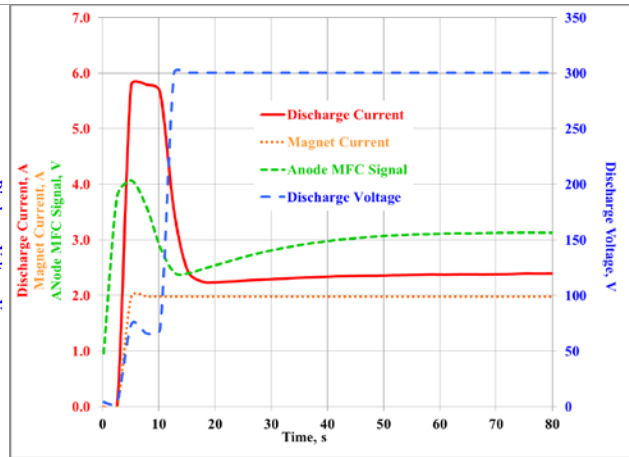


**Figure 6. Plot of the HiVHAc thruster glow mode discharge initiation transient.**

Figure 7 shows the PPU throttling profile of the HiVHAc thruster from low power to higher power and then back to lower power. As the thruster power is ramped up from 1.5 kW to 3.5 kW at a constant discharge voltage, a slight overshoot occurs in the discharge current, but the feedback loop lowers the anode flow rate to reach the prescribed discharge current value. After testing at 3.5 kW and 500V, the thruster was transitioned to 3.9 kW and 650 V, as is shown in Fig.7. Then, the thruster was transitioned to lower power by setting lower discharge current values.

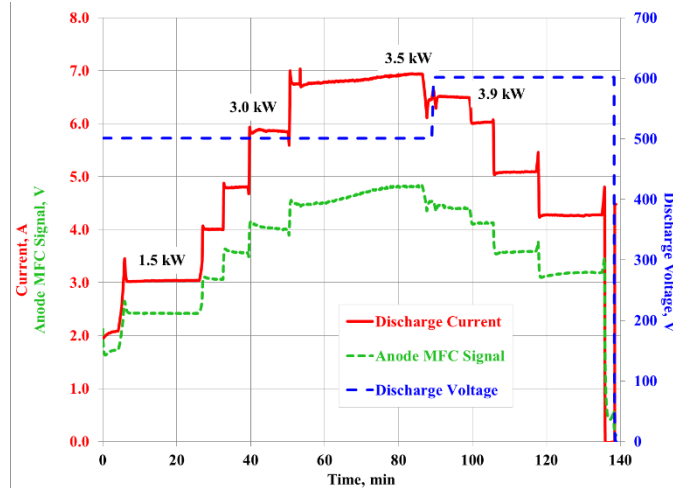


**Figure 7. HiVHAc thruster throttling profile with discharge current regulation via anode flow control.**

#### IV. SPT-140 Thruster Integration Test Results

Tests of the SPT-140 thruster were also performed in VF12 as is shown in Fig 2. However, for the SPT-140 tests the PPU was installed in Vacuum Facility 70 (VF70) and was mounted on a liquid-cooled baseplate. VF70 is a 0.5 m diameter by 1 m long vacuum chamber located adjacent to VF12 for PPU testing. It is capable of maintaining a base pressure less than  $1 \times 10^{-6}$  Torr during full power PPU operation. Prior to testing with the SPT-140, the EM PPU was baked-out and then subjected to a vacuum functional and performance test as is reported in Reference 1.

For the SPT-140 test, electromagnet settings provided by SSL were used for thruster operation at 1.5 kW and 4.5 kW power levels.<sup>12</sup> During thruster operation at different discharge current and voltage conditions, very limited electromagnet tuning was performed during steady state thruster operation, and no attempts were made to optimize the thruster performance.

The SPT-140 test was performed in two segments. In segment 1, the PPU was operated in open-loop mode where the XFCM was not used to regulate the flow to the thruster and MFCs were used to provide the regulated flow to the thruster. In segment 2, closed-loop operation of the thruster was performed where the PPU was used to initiate the cathode heating, initiate the thruster discharge, maintain steady state operation, and throttle the thruster to the set throttle point. For both segments 1 and 2, the cathode flow rate was manually set to 7% of the anode flow.

In segment 1, the thruster operation and performance were characterized over a range of discharge currents and voltages. The thruster was operated at discharge voltages between 200 and 600 V and at discharge currents between 5 and 15 A. In segment 2, the thruster was operated at discharge voltages between 200 and 600 V but the discharge current was limited to between 5 and 9 A. Attempts to throttle to higher discharge currents were not successful due to the DCIU feedback loop parameters not being optimized. Figure 8 presents the SPT-140 thruster throttle conditions tested in VF12. Figure 9 shows a photograph of the thruster operating at 4500 W.

Figure 10 presents the thruster startup sequence. For the SPT-140 test series, the thruster was started in Hall mode. After completing the cathode ignition heating cycle, a cathode keeper current of 2 A was applied, then the anode flow was initiated and the keeper current was reduced to 0.5 A. Then, the discharge voltage and the magnet current were energized, resulting in the thruster discharge current initiation. Following the discharge current initiation, the anode flow rate continued to ramp up at a slow rate for approximately 30 s, while at the same time the magnet current ramp rate was increased. After approximately 50 s, the thruster's discharge current reached its target steady state value.

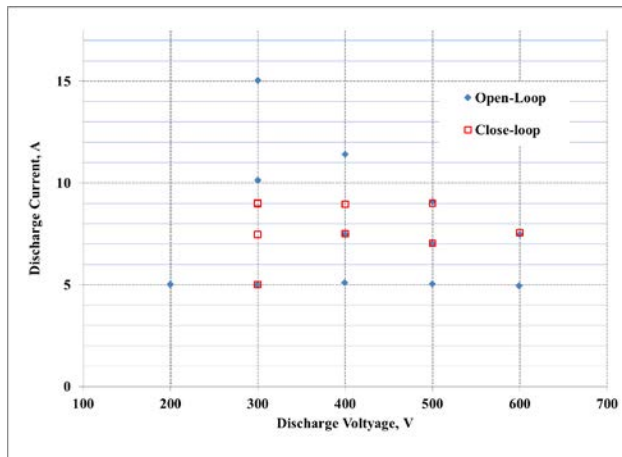


Figure 8. SPT-140 nominal operating throttle points during open and closed-loop tests with the CPE EM PPU and VACCO's XFCM.

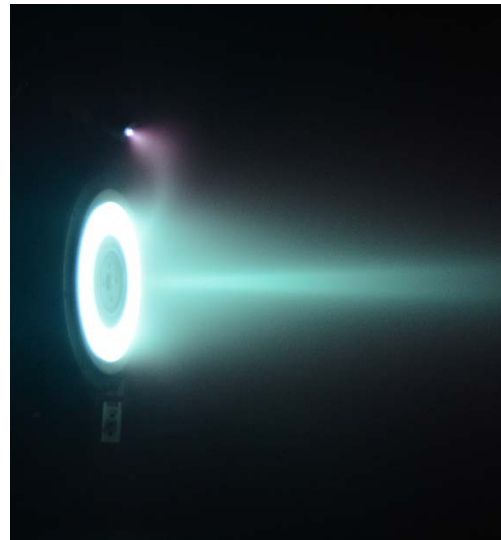


Figure 9. Photograph of the SPT-140 during tests at 4.5 kW in NASA GRC's VF12.

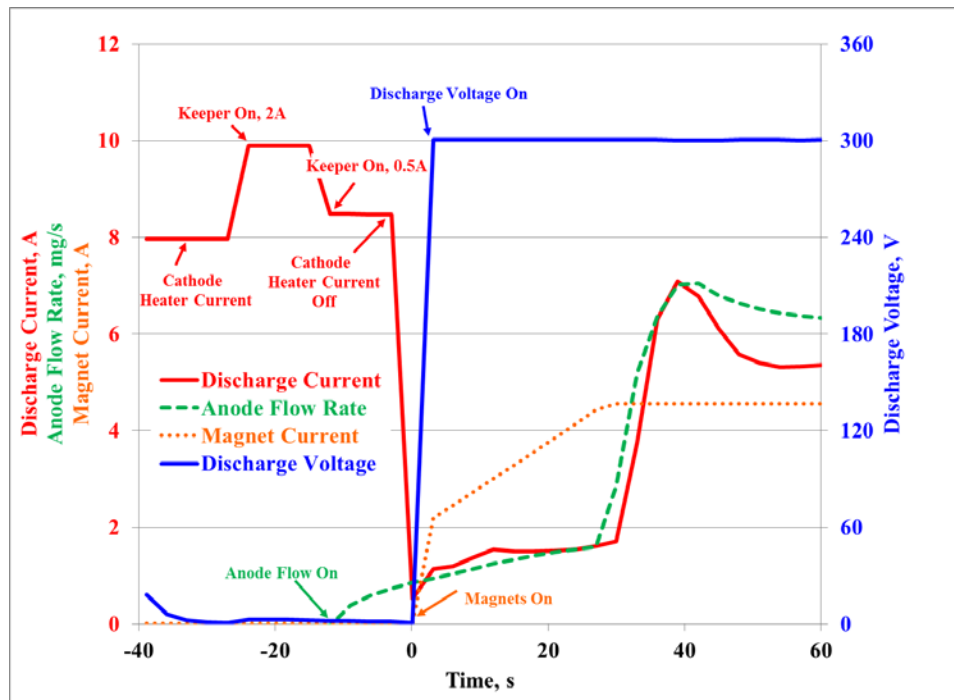


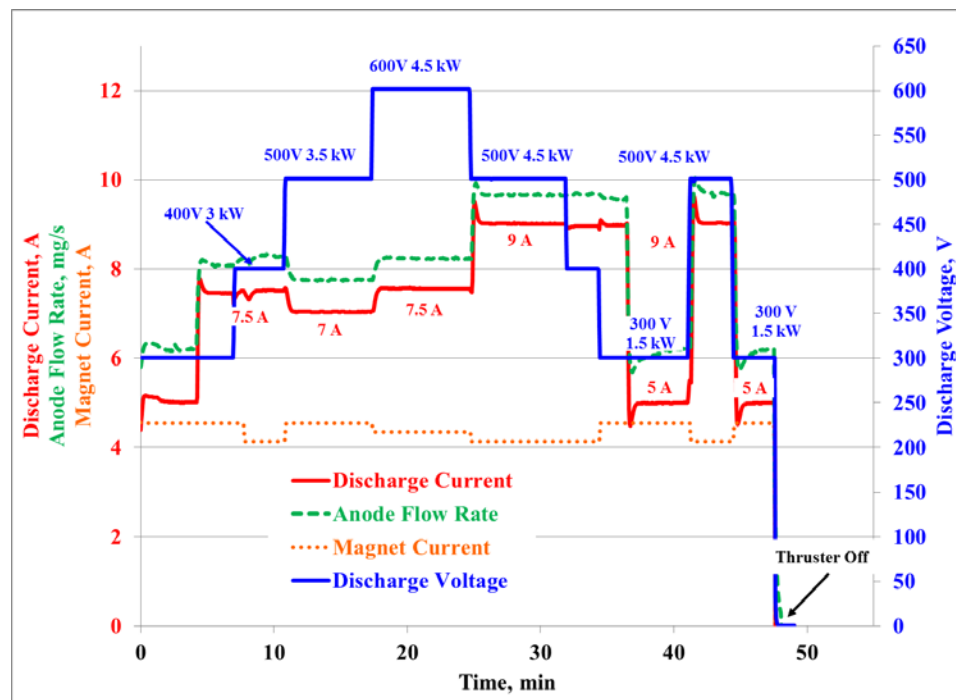
Figure 10. The SPT-140 thruster startup sequence with the EM PPU and XFCM.

Figure 11 shows the thruster throttling profiles during segment 2 operation. The thruster discharge was initiated at a discharge voltage of 300 V and discharge current of 5 A, as is shown in Fig. 10. The thruster discharge was then throttled from 1.5 kW to 4.5 kW then back to 1.5 kW as is shown in Fig. 11 and Table 3:

**Table 3. Summary of the SPT-140 throttling profiles during closed-loop operation**

Test Point #	Thruster Discharge Operating Condition	Discharge Power, kW
1	300 V, 5 A	1.5
2	300 V, 7.5 A	2.25
3	400 V, 7.5 A	3.0
4	500 V, 7 A	3.5
5	600 V, 7.5 A	4.5
6	500 V, 9 A	4.5
7	400 V, 9 A	3.6
8	300 V, 9 A	2.7
9	300 V, 5 A	1.5
10	300 V, 9 A	2.7
11	300 V, 5 A	1.5
	OFF	

Attempts to operate in closed-loop mode at currents of 10 A and above were not successful due to the DCIU feedback loop parameters not being optimized. Future development of the CPE EM PPU are reported in Reference 6.



**Figure 11. SPT-140 throttling profile during closed-loop operation with EM PPU and XFCM.**



Figure 12 presents the SPT-140 thrust at the different thruster operating conditions. At a discharge voltage of 300 V, thrust levels of 193 mN and 281 mN were measured at discharge currents of 10.1 and 15.05 A, respectively. At a discharge voltage of 300 V, SSL reported thrust levels of 191 mN and 282 mN at discharge currents of 10 A and 15 A, respectively.<sup>12</sup> The identical thrust values indicate that the SPT-140 DM4 thruster was operating nominally when being powered by the CPE EM PPU. Figure 12 also presents the thrust levels that were generated during segment 2 test, which show consistency in the thrust levels between the two segments.

Figures 13 and 14 present the total thrust efficiency and specific impulse magnitudes during segments 1 and 2. Results in Figs. 13 and 14 show performance levels that are similar to what has been reported by SSL and Snyder.<sup>12,13,14</sup> Additionally, comparison of segment 1 and 2 results indicated almost identical performance levels, further confirming that the thruster's closed-loop operation results in similar thruster operation as open-loop operation.

Table 4 presents a summary of the ratio of the discharge current, anode flow rate, and thrust between open-loop and closed-loop thruster operation. Results in Table 4 indicate that the ratios were between 0.99 and 1.02; this is within the respective measurements uncertainty.

**Table 4. Ratio of SPT-140 discharge current, anode flow rate, and thrust during open and closed-loop operation.**

Operating Condition	$\frac{I_{d_{closed-loop}}}{I_{d_{open-loop}}}$	$\frac{\dot{m}_{a_{closed-loop}}}{\dot{m}_{a_{open-loop}}}$	$\frac{Thrust_{closed-loop}}{Thrust_{open-loop}}$
300 V, 1.5 kW	1.00	1.00	1.02
400 V, 3.0 kW	1.00	1.00	1.01
500 V, 3.5 kW	1.00	0.99	1.02
500 V, 4.5 kW	0.99	0.99	1.00

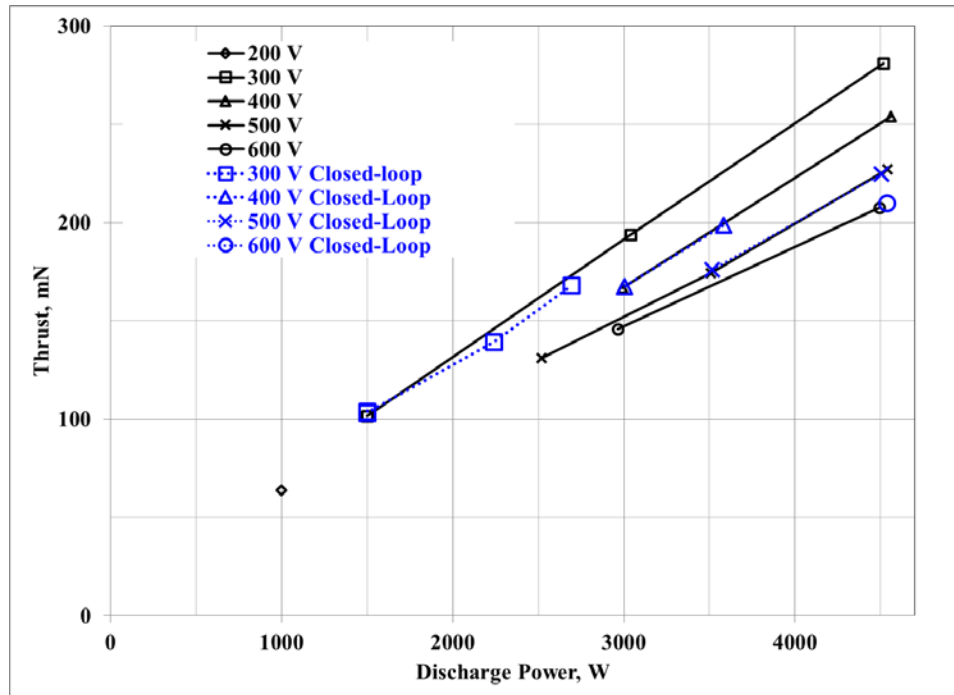


**Figure 12. SPT-140 thrust levels during open and closed-loop operation with the EM PPU and XFCM.**

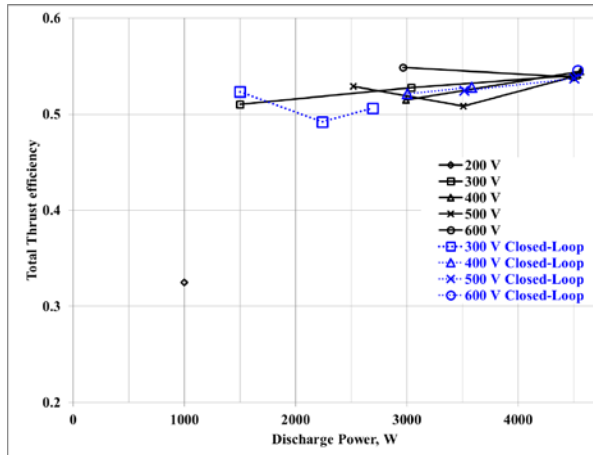


**Figure 13. SPT-140 total thrust efficiency during open and closed-loop operation with EM PPU and XFCM.**

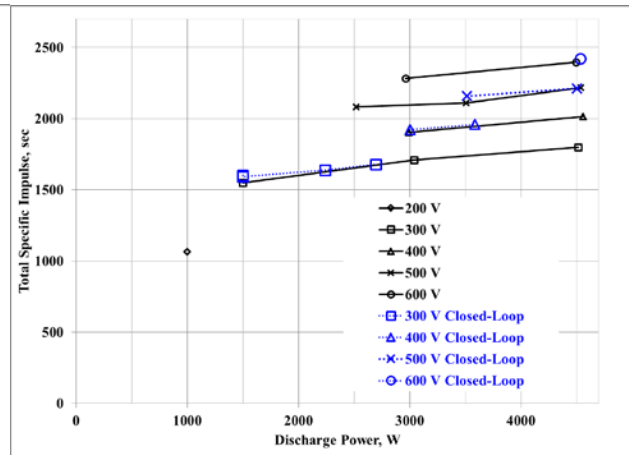


**Figure 14. SPT-140 total specific impulse during open and closed-loop operation with EM PPU and XFCM.**

Figure 15 presents the measured root mean square (RMS) discharge current oscillations. The values were within 10% of the mean discharge current except for thruster operation at 400 V and 600 V at 7.5 A. At a discharge voltage of 300 V, the RMS oscillation levels matched levels reported by Snyder.<sup>13</sup> At discharge voltage levels of 400 and 600 V, the RMS oscillation levels were higher than what was reported by Snyder, but the differences are mainly attributed to the fact that magnet tuning was not performed during this study and that the electrical filter configuration for this test was different than what was used in the earlier study. Figure 16 presents the power spectral density (PSD) profiles for the thruster operating at 300, 400, 500, and 600 V. At 300 V the PSDs indicate a similar profile for discharge currents of 5, 10, and 15 A, although with different magnitudes at slightly different frequencies. At 400-600 V, the PSDs show similar profiles that are different than 300 V. At voltages above 300 V, two pronounced peaks exist in the PSD. Table 5 lists the frequencies at peak PSDs for the different operating conditions. For all discharge voltages, the first peak occurs between 25 and 30 kHz which is similar to what was reported by Snyder;<sup>13</sup> whereas, for discharge voltages of 400 to 600 V, the second peak occurs at a frequency of ~50-60 kHz. Results presented in Fig. 16 and Table 5 indicate that the thruster changed modes when operating at discharge voltages above 300 V and that the PPU (with a non-optimized filter and minimum magnet tuning) was able to power the discharge without any reductions or variations in thruster performance.

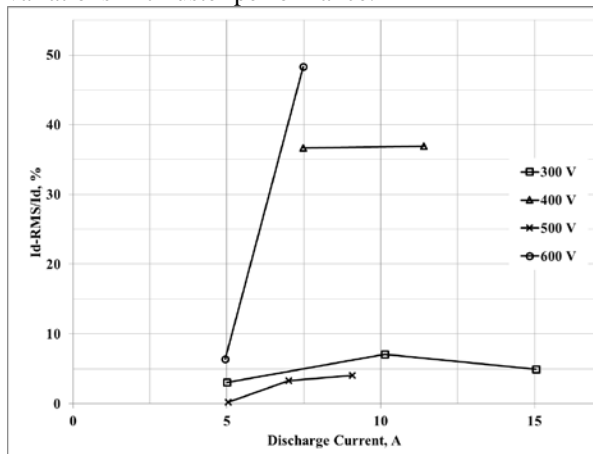


**Figure 15. SPT-140 discharge current RMS to discharge current at various thruster operating power levels.**

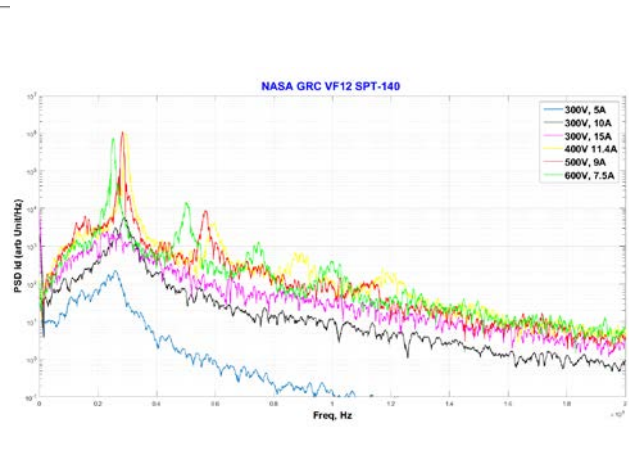


**Figure 16. SPT-140 PSDs for various thruster operating power levels.**

**Table 5. Summary of the SPT-140 PSDs analysis showing the peak PSD magnitudes and frequencies.**

<b>Operating Condition</b>	<b>Peak Magnitude</b>	<b>Frequency, kHz</b>
300 V 5 A	223	25.9
300 V 10 A	5725	28.8
300 V 15 A	2498	22.9
	1363	31.4
400 V 11.4 A	983637	29.6
	4179	59.9
500 V 9.1 A	1062963	28.3
	8870	56.7
600 V 7.5 A	736709	25.3
	14776	49.9
	1304	74.7

## **V. Summary and Future Work**

The development of the HiVHAc Hall thruster propulsion system is an on-going effort. The primary components of the HiVHAc propulsion system include the HiVHAc thruster, the CPE PPU, and the VACCO XFCM unit. The CPE EM PPU is designed to have a variable input voltage range between 80 and 160 V, and a wide output voltage range between 200 and 700 V.

Integrated tests of the HiVHAc EDU thruster were performed with the EM PPU and the XFCM unit. The HiVHAc integrated test demonstrated that the EM PPU DCIU and programmed algorithms were able to heat the cathode, initiate the cathode discharge, initiate the thruster discharge (in two modes), operate the thruster in steady state, and throttle the thruster.

Integrated tests of the SPT-140 with the EM PPU and XFCM unit were performed to demonstrate the versatility of the EM PPU and XFCM. The integrated test of the SPT-140 with the EM PPU and VACCO XFCM resulted in nominal thruster operation. The SPT-140 integrated test demonstrated that the EM PPU DCIU and programmed algorithms were able to heat the cathode, initiate the cathode discharge, initiate the thruster discharge (in two modes), operate the thruster in steady state, and throttle the thruster. The measured SPT-140 thruster performance was identical to values reported by SSL. The thruster performance during open and closed-loop operation also indicated identical thruster operation. The SPT-140 discharge current waveform oscillations at 300 V were identical to previously reported values.

Tests of the EM PPU and the VACCO XFCM did uncover some further refinements that have to be performed to the PPU DCIU algorithms and they include:

- Incorporation of another option for thruster start up to allow for a soft thruster discharge initiation in Hall mode;
- Refinement of the discharge current-anode flow rate feedback control loop parameters to enable closed-loop control for thruster operation at discharge currents above 10 A; and
- Incorporation of another feedback loop on the cathode flow to allow for closed-loop regulation of the cathode flow rate.

Finally, the NASA GRC led team, which includes JPL, is continuing to further mature the CPE PPU hardware. A prototype development unit (PDU) is under development by CPE with funding from NASA's SBIR Program office, NASA's Science Mission Directorate, NASA's Space Technology Mission Directorate, NASA GRC, and NASA JPL. The PDU PPU will include several changes to input and output specifications to allow operation of other thrusters. The PDU PPU will also include additional functionality typically expected in flight Hall thruster systems and is expected to be completed in late 2018.

## Acknowledgments

The authors would like to thank and acknowledge the Science Mission Directorate, NASA Space Technology mission Directorate, NASA SBIR program, and NASA Glenn for supporting the CPE PPU development and testing. The support of Carol Tolbert and Todd Peterson is acknowledged and appreciated. Lastly, the authors would like to thank Kevin Blake, George Jacynycz, and Michael McVetta for supporting the assembly and installation of the thruster and PPU in the vacuum test facilities, as well as maintaining and operating the vacuum facilities.

## References

- <sup>1</sup> Dankanich, J. W., "Electric Propulsion for Small Body Missions", AIAA Paper 2010-6614, August 2010.
- <sup>2</sup> Brophy, J., Garner, C., Nakazono, B., Marcucci, M., Henry, M., and Noon, D., "The ion Propulsion System for Dawn," AIAA-2003-4542, July, 2003.
- <sup>3</sup> Garner, C.E., Rayman, M.D., and Brophy, J.R., "In-Flight Operation of the Dawn Ion Propulsion System Through Year One of the Cruise to Ceres," AIAA-2013-4112, July 2013.
- <sup>4</sup> Dankanich, J.W., Drexler, J. A., and Oleson, S. R., "Electric Propulsion Mission Viability with the Discovery-Class Cost Cap," AIAA Paper 2010-6776, August 2010.
- <sup>5</sup> Pinero, L. R., Kamhawi, H., and Drummond, G., "Integration Testing of a Modular Discharge Supply for NASA's High Voltage Hall Accelerator Thruster," IEPC Paper 2009-275, September 2009.
- <sup>6</sup> Pinero, L.R., Kamhawi, H., and Shilo, V., "Performance of a High-Fidelity 4 kW-Class Engineering Model PPU and Integration with HiVHAc System," presented in the 52<sup>nd</sup> AIAA/SAE/ASEE Joint Propulsion Conference, Salt Lake City, Utah, July 2016.
- <sup>7</sup> Dankanich, J., Cardin, J., Dien, A., Kamhawi, H., Netwall, C., and Osborn, M., "Advanced Xenon Feed System (AXFS) Development and Hot-fire Testing," 45<sup>th</sup> AIAA Joint Propulsion Conference, AIAA 2009-4910, Denver, Colorado, USA, August 2-5, 2009.
- <sup>8</sup> Kamhawi, H., *et al.*, "Performance and Environmental Test Results of the High Voltage Hall Accelerator Engineering Development Unit," AIAA 2012-3854, July 2012.
- <sup>9</sup> Manzella, D.H., J. Hamley, J. Miller, C. Clauss, K. Kozubsky, and R. Gnizdor, "Operational Characteristics of the SPT-140 Hall Thruster," AIAA 1997-2919, 33<sup>rd</sup> Joint Propulsion Conference, Seattle, WA, July, 1997.
- <sup>10</sup> Manzella, D.H., C. Sarmiento, J. Sankovic, and T. Haag, "Performance Evaluation of the SPT-140," IEPC 1997-059, 25<sup>th</sup> International Electric Propulsion Conference, Cleveland, OH, August 24-28, 2007.
- <sup>11</sup> Kamhawi, H., Haag, T., Huang, W., Pinero, L., Peterson, T., and Dankanich, J., "Integration Tests of the High Voltage Hall Accelerator System Components at NASA Glenn Research Center," 33<sup>rd</sup> International Electric Propulsion Conference, IEPC-2013-445, Washington, DC, 6-10 Oct., 2013.
- <sup>12</sup> Personal Communication, Liang, R., Space Systems Loral, April 2016.
- <sup>13</sup> Snyder, J. S., and Hofer, R. R., "Throttled Performance of the SPT-140 Hall Thruster," AIAA-2014-3816, July 2014.
- <sup>14</sup> Garner C., Jorns B. A., Derventer S. V., Hofer R. R., Ryan R., Liang R., and Delgado J., "Low-Power Operation and Plasma Characterization of a Qualification Model SPT-140 Hall Thruster for NASA Science Missions," AIAA-2015-3720, July 2015.